AFRL-RD-PS-
TP-2015-0004

AFRL-RD-PS-
TP-2015-0004

EXPERIMENTAL AND THEORETICAL STUDIES OF PHASE MODULATION IN Yb-DOPED FIBER AMPLIFIERS (POSTPRINT)

Angel Flores, et al.

1 April 2012

Technical Paper

APPROVED FOR PUBLIC RELEASE; DISTRIBUTION IS UNLIMITED.

AIR FORCE RESEARCH LABORATORY
Directed Energy Directorate
3550 Aberdeen Ave SE
AIR FORCE MATERIEL COMMAND
KIRTLAND AIR FORCE BASE, NM 87117-5776

REPORT DOCUMENTATION PAGE	*Form Approved* *OMB No. 0704-0188*

1. REPORT DATE *(DD-MM-YYYY)*	**2. REPORT TYPE**	**3. DATES COVERED** *(From - To)*
01/04/2012	Technical Paper	1 April 2012

4. TITLE AND SUBTITLE Experimental and Theoretical Studies of Phase Modulation in Yb-doped Fiber Amplifiers(Postprint)	**5a. CONTRACT NUMBER** **5b. GRANT NUMBER** **5c. PROGRAM ELEMENT NUMBER**
6. AUTHOR(S) Angel Flores, Chunte Lu, Craig Robin, Shadi Naderi, Christopher Vergien, Iyad Dajani	**5d. PROJECT NUMBER** **5e. TASK NUMBER** **5f. WORK UNIT NUMBER** D061
7. PERFORMING ORGANIZATION NAME(S) AND ADDRESS(ES) Air Force Research Laboratory 3550 Aberdeen Ave SE Kirtland AFB, NM 87117-5776	**8. PERFORMING ORGANIZATION REPORT NUMBER**
9. SPONSORING / MONITORING AGENCY NAME(S) AND ADDRESS(ES) Air Force Research Laboratory 3550 Aberdeen Ave SE Kirtland AFB, NM 87117-5776	**10. SPONSOR/MONITOR'S ACRONYM(S)** AFRL/RDLT **11. SPONSOR/MONITOR'S REPORT NUMBER(S)** AFRL-RD-PS-TP-2015-0004

12. DISTRIBUTION / AVAILABILITY STATEMENT

Approved for public release: distribution unlimited. 377ABW-2012-0571; 15 May 2012.

13. SUPPLEMENTARY NOTES

Accepted for publication in the SPIE Proceedings; A. Flores, C. Lu, C. Robin, S. Naderi, C. Vergien, and I. Dajani, "Experimental and theoretical studies of phase modulation in Yb-doped fiber amplifiers," Proc. SPIE 8381, 83811B1 (2012). Presented at SPIE Defense and Security 2012, Baltimore, MD, (April 2012) "Government Purpose Rights"

14. ABSTRACT

We present detailed studies of the effect of sinusoidal phase modulation on stimulated Brillouin scattering (SBS) in ytterbium-doped fiber amplifiers. Based on a time-dependent SBS model, SBS enhancement factor versus pump linewidth for different modulation depths ranging from 0 to, and modulation frequencies ranging from 30 MHz to 500 MHz were analyzed. In addition, experimental validation of SBS suppression via sinusoidal phase modulation is presented with experimental results agreeing well with the model and simulations. Furthermore, narrow linewidth coherent beam combining (CBC) of 5 sinusoidal phase modulated lasers is demonstrated via LOCSET.

15. SUBJECT TERMS

Yb-doped fiber lasers, Stimulated Brillouin scattering, nonlinear optics

16. SECURITY CLASSIFICATION OF:			**17. LIMITATION OF ABSTRACT**	**18. NUMBER OF PAGES**	**19a. NAME OF RESPONSIBLE PERSON**
					Angel Flores
a. REPORT	**b. ABSTRACT**	**c. THIS PAGE**	SAR	11	**19b. TELEPHONE NUMBER** *(include area code)*
Unclassified	Unclassified	Unclassified			505-846-4517

Standard Form 298 (Rev. 8-98)
Prescribed by ANSI Std. 239.18

Experimental and theoretical studies of phase modulation in Yb-doped fiber amplifiers

Angel Flores, Chunte Lu, Craig Robin, Shadi Naderi, Christopher Vergien and Iyad Dajani
Air Force Research Laboratory, 3550 Aberdeen Ave SE, Kirtland AFB, NM, USA 87117-0001

ABSTRACT

We present detailed studies of the effect of sinusoidal phase modulation on stimulated Brillouin scattering (SBS) in ytterbium-doped fiber amplifiers. Based on a time-dependent SBS model, SBS enhancement factor versus pump linewidth for different modulation depths ranging from 0 to π, and modulation frequencies ranging from 30 MHz to 500 MHz were analyzed. In addition, experimental validation of SBS suppression via sinusoidal phase modulation is presented with experimental results agreeing well with the model and simulations. Furthermore, narrow linewidth coherent beam combining (CBC) of 5 sinusoidal phase modulated lasers is demonstrated via LOCSET.

Keywords: Yb-doped fiber lasers, Stimulated Brillouin scattering, nonlinear optics

1. INTRODUCTION

Fiber lasers offer several advantages over conventional solid state lasers and chemical lasers; including compactness, near diffraction-limited beam quality, superior thermal-optical properties, and high output efficiencies. However, due to small core sizes and long amplifier lengths; high-power, single-mode fiber lasers are limited by the onset of (power-dependent) detrimental effects, such as SBS. It is well-known that power scaling in single and narrow linewidth fiber amplifiers is primarily limited by SBS. This process is a third-order phase-matched nonlinear interaction that couples acoustic phonons to photons of the optical field and the associated backscattered Stokes light. Consequently, optical power is transferred from the laser field and into the Stokes light; thus degrading amplification of the signal light and possibly damaging the fiber amplifier through pulsation. The limiting power level is commonly referred to as the SBS threshold. In this paper, we define the SBS threshold to be the point at which the time-averaged reflectivity measured over several transit time reaches 1%.

Typical SBS mitigation techniques include decreasing the fiber effective length, L_{eff}, which is limited by solubility limits of ytterbium as well as associated photodarkening effects. Similarly, power scaling in single-frequency fiber amplifiers has been achieved through large mode area (LMA) fibers coiled to filter out higher order modes [1]. Another fundamental SBS mitigation technique revolves around spectral linewidth broadening [2]. The linewidth broadening is commonly achieved through RF phase modulation and suppression occurs when the phase variation is on a time scale shorter than the phonon lifetime. If the effective coherence length of the laser is much shorter than the SBS interaction length, considerable SBS suppression can be achieved. In this case, the suppression factor is given by [3]:

$$\frac{P_{th}^{m}}{P_{th}^{0}} = 1 + \frac{\Delta\nu_l}{\nu_B} \ , \qquad (1)$$

where $\Delta\nu_l$ and $\Delta\nu_B = \Gamma_B / 2\pi$ are the laser and Brillouin spectral widths, respectively, and where P_{th}^{m} and P_{th}^{0} are the power outputs at SBS threshold for the modulated and single-frequency cases, respectively. However, recent demonstrations of a kW class fiber amplifier had a measured linewidth of 11 GHz [4]. According to Eq. [1], with an 11 GHz linewidth and spontaneous Brillouin linewidth of ~60 MHz, the SBS threshold should increase by a factor of ~200 and produce much higher multi-kW power levels. To help explain such deviations, we have investigated and developed time-dependent nonlinear models for simulation of phase modulated high-power fiber lasers [5].

The time-dependent SBS process was treated previously in passive fiber [6]. However, this research did not consider phase-modulation of the pump input. An analytic formula for the Stokes light in the long-time limit for an undepleted pump has also been developed [7]. Nevertheless, this work is based on the assumption that the laser field

is constant in both time and space and may not be applicable for phase modulated pumps. The SBS process has also been studied with phase modulation in the Fourier domain [8], but the model was developed for long haul fiber (> 1 km). In this case, the phase mismatched terms arising from Stokes sidebands interactions (created through phase modulation) may be neglected. Since most fiber amplifiers have moderate interaction lengths (L~10 m), these approximations may not be valid and cause discrepancies in high-power fiber amplifiers. In contrast, our time-dependent SBS model studies the effects of phase modulation with no assumption on fiber length, separation between optical sidebands, or pump depletion effects. Subsequently, in this report we present detailed studies of the effect of sinusoidal phase modulation on SBS in ytterbium-doped fiber amplifiers. Here SBS suppression is compared in relation to modulation depth ranging from 0 to π and modulation frequency ranging from 30 MHz to 500 MHz. More importantly, we compare experimental results to the theoretical predictions of our time-dependent model for the sinusoidal modulation case. Furthermore, we demonstrate CBC of five narrow linewidth sinusoidal modulated fiber lasers.

2. TIME-DEPENDENT MODEL

The SBS process is examined using a triply coupled set of partial differential equations which describes a three-wave interaction of two optical fields and an acoustic field. These equations are derived from Maxwell's equations and the Navier-Stokes equations. The laser field, $\tilde{E}_L$, the Stokes field, $\tilde{E}_S$, and the acoustic phonon field, $\tilde{\rho}$, are represented as time-harmonic monochromatic plane waves:

$$\tilde{E}_L = A_L(z,t)e^{i(k_L z-\omega_L t)} + c.c. \tag{2}$$

$$\tilde{E}_S = A_S(z,t)e^{i(-k_S z-\omega_S t)} + c.c. \tag{3}$$

$$\tilde{\rho} = \rho_O + \rho(z,t)e^{i(qz-\Omega t)} + c.c. \tag{4}$$

where A_L, A_S, and ρ represent the amplitudes of oscillations of the pump, Stokes, and acoustic fields, respectively. Here k_L, k_S, and q represent the pump, Stokes, and acoustic wave numbers; and ω_L, ω_S, and Ω represent the pump, Stokes, and acoustic angular frequencies. ρ_0 is the background density of the fiber medium. Accordingly, conservation of energy and momentum dictate that the acoustic and optical wave numbers and angular frequencies are related through: $\Omega = \omega_L - \omega_S$ and $q = k_L + k_S$.

Hence, the total optical field, $\tilde{E} = \tilde{E}_L - \tilde{E}_S$, can be described by the nonlinear wave equation:

$$\nabla^2 \tilde{E} - \frac{n^2}{c^2}\frac{\partial^2 \tilde{E}}{\partial t^2} = \frac{1}{\varepsilon_o c^2}\frac{\partial^2 \tilde{P}^{(nl)}}{\partial t^2} \quad , \tag{5}$$

where the nonlinear polarization, $\tilde{P}^{(nl)}$, is due to the modification of the index of refraction as a result of electrostriction and is given by $\tilde{P}^{(nl)} = \varepsilon_0 \gamma_\varepsilon \tilde{\rho}\tilde{E} / \rho_0$. The electrostrictive constant, γ_ε, describes the change in the dielectric constant of the medium, ε, with respect to a change in density and is given by $\gamma_\varepsilon = \rho(\partial\varepsilon / \partial\rho)$. Similarly, the evolution of the acoustic field is described by the wave equation [5]:

$$\frac{\partial^2 \tilde{\rho}}{\partial t^2} - \frac{\Gamma_B}{q^2}\nabla^2 \frac{\partial \tilde{\rho}}{\partial t} - v_S^2 \nabla^2 \tilde{\rho} = -\frac{1}{2}\varepsilon_o \gamma_e \nabla^2 \left\langle \tilde{E}^2 \right\rangle + \tilde{f} \quad , \tag{6}$$

where Γ_B is the phonon decay rate and υ_s is the speed of sound. For the first term on the RHS of Eq. (6), only the product of the form $E_L E_S^*$ is pertinent. The second term accounts for the initiation of the SBS process from a Langevin noise source, which can be expressed as:

$$\tilde{f} = -2i\Omega f(z,t)e^{i(qz-\Omega t)} + c.c. \; , \tag{7}$$

where f is a Gaussian random variable with zero mean and is δ correlated in space and time.

Substituting the total optical field into Eq. (5), and using the slowly-varying envelope approximation, one can obtain the equations which describe the evolution of the optical field amplitudes in the fiber:

$$\frac{c}{n}\frac{\partial A_L}{\partial z} + \frac{\partial A_L}{\partial t} = \frac{i\omega\gamma_e}{2n^2\rho_o}\rho A_S \tag{8}$$

$$-\frac{c}{n}\frac{\partial A_S}{\partial z} + \frac{\partial A_S}{\partial t} = \frac{i\omega\gamma_e}{2n^2\rho_o}\rho^* A_L \tag{9}$$

where $\omega \approx \omega_L \approx \omega_S$. In particular, phase modulation effects are included through the initial and boundary for the electric field at the input end of the fiber:

$$A_L(0,t) = A_L^0 e^{i\varphi(t)} \tag{10}$$

$$A_L(z>0,0) = 0 \; , \tag{11}$$

where $\varphi(t)$ is the phase modulation function and A_L^0 describes the input electric field amplitude of the pump. The Stokes field is counter-propagating and is zero everywhere at $t = 0$. It is subject to the following conditions, $A_S(z,0) = 0$ & $A_S(L,0) = 0$, where L is the length of the fiber.

Since the phonons are highly damped, they propagate over very short distances. Consequently, in the phonon equation, the spatial variation of the amplitude is neglected leading to:

$$\frac{\partial^2\rho}{\partial t^2} + \left(\Gamma_B - 2i\Omega\right)\frac{\partial\rho}{\partial t} + \left(\Omega_B{}^2 - \Omega^2 - i\Omega\Gamma_B\right)\rho = \varepsilon_o\gamma_e q^2 A_L A_S^* - 2i\Omega f \tag{12}$$

where we have introduced the resonant acoustic frequency of the medium, $\Omega_B = 2nv_S\omega_L / c$. We note that in absence of external effects (stress, fiber impurities, temperature variations), we can solve Eq. (12) at resonance ($\Omega = \Omega_B$):

$$\frac{\partial^2\rho}{\partial t^2} + \left(\Gamma_B - 2i\Omega_B\right)\frac{\partial\rho}{\partial t} - i\Omega_B\Gamma_B\rho = \varepsilon_o\gamma_e q^2 A_L A_S^* - 2i\Omega_B f \; . \tag{13}$$

Equations (8), (9), and (13), along with the boundary and initial conditions completely describe the three-wave interaction including the initiation of the SBS process from noise. Subsequently, to study the effects of a phase-modulated pump at high reflectivity, we perform numerical integration of the coupled set of equations using the method of characteristics [5].

3. SINUSOIDAL PHASE MODULATION

To validate our time-dependent model we explore SBS suppression due to single-frequency sinusoidal phase modulation with mod depth γ and modulation frequency ω_{FM}. Accordingly, the modulation function is given by:

$$\varphi(t) = \gamma \sin(\omega_{FM} t) \tag{14}$$

Here the time dependence of the input electric field exhibits the following form:

$$\tilde{E}_L(0,t) = A_L^0 \begin{bmatrix} J_0(\gamma)\cos(\omega t) + J_1(\gamma)\cos(\omega + \omega_{FM})t - J_1(\gamma)\cos(\omega - \omega_{FM})t \\ + J_1(\gamma)\cos(\omega + 2\omega_{FM})t - J_1(\gamma)\cos(\omega - 2\omega_{FM})t + ... \end{bmatrix} \tag{15}$$

As a result, the spectral power exhibits a series of discrete sidebands at integer multiples of the modulation frequency. The power spectral density (PSD) of the nth sideband is given as:

$$P_{L,n} \propto J_n^2(\gamma) \tag{16}$$

where J_n is the n^{th} order Bessel function of the first kind. For example, Figure 1 shows the PSD of an optical field phase-modulated according to Eq. (14) where $\gamma = 1.435$ radians and $\omega_{FM} = 2\Gamma_B$. Using Eq. (15), one may verify that this specific modulation depth results in three equal intensity lobes near the center of the spectrum.

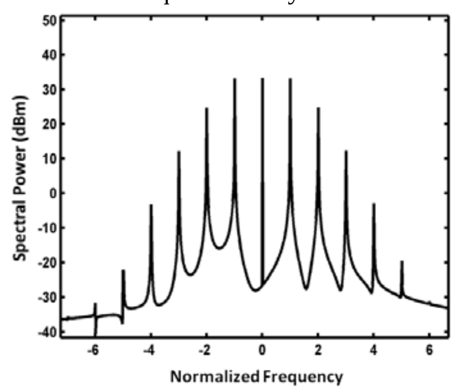

Figure 1. PSD of the pump phase modulated with a single-sinusoidal modulation function for the case $\gamma = 1.435$ and $\omega_{FM} = 2\Gamma_B$. The normalized frequency represents the shift from the carrier frequency divided by the modulation frequency.

Subsequently, we characterize the SBS threshold as a function of phase modulation amplitude and frequency for a specific fiber length of 5 m and a core diameter of 10 µm. In all cases, we define the SBS threshold as the input field power for which the time-averaged reflectivity over several transit times (where the transit time is given by $\tau_{RT} = nL/c$) is ~1%. In addition, the total simulation time encapsulated at least 20 transit times. The SBS threshold enhancement normalized to the un-modulated threshold is shown in Figure 2 for various combinations of γ and ω_{FM} using typical fiber parameters [5]. The x-axis in the figure is normalized to the spontaneous Brillouin bandwidth. An analytical expression for the SBS threshold can be obtained using a heuristic treatment in the frequency domain. For large modulation frequencies, $\omega_{FM} >> \Gamma_B$, the Stokes modes resulting from the phase modulation of the optical field act independently and the SBS threshold is determined by the sideband with the highest spectral power. To that end the SBS threshold enhancement factor as compared to an un-modulated wave is given by:

$$P_{th} / P_{th}^0 = \frac{1}{J_{n,\max}^2(\gamma)} \tag{17}$$

where P_{th} is the SBS threshold, P_{th}^0 is the SBS threshold for the case of an un-modulated field, and $J_{n,\max}(y)$ is the Bessel function of the 1st kind corresponding to the sideband with the maximum value. The SBS enhancement factor as provided by Eq. (17) is plotted in Figure 2 for comparison to the numerical simulations.

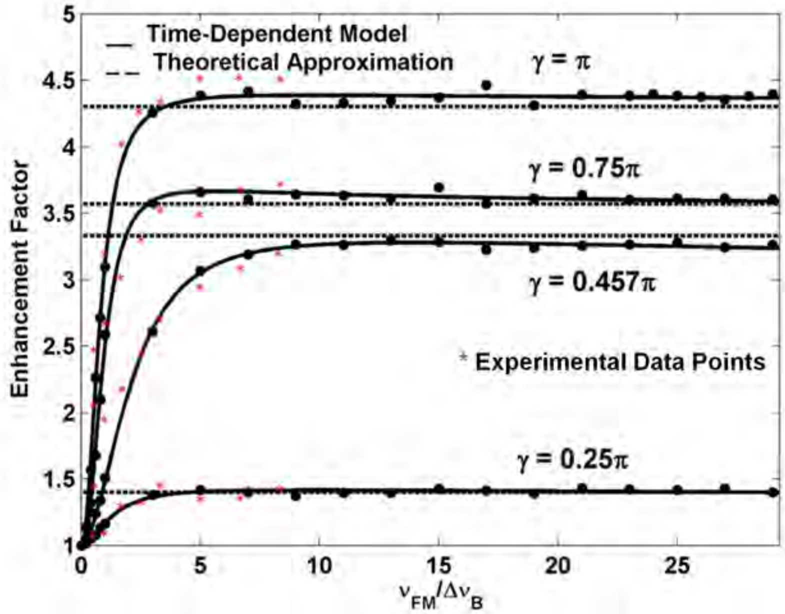

Figure 2. Numerical results (solid dots) of SBS threshold enhancement factor vs. normalized modulation frequency for various modulation amplitudes. Solid curves represent best fit for numerical results and red dots depict experimental data points. As expected, the results indicate asymptotic convergence to the theoretical approximation of Eq. (17) in the large modulation frequency limit. More importantly, experimental data is in good agreement with time-dependent model.

Moreover, to further validate the numerical models experimental validation of SBS suppression through sinusoidal phase modulation has been performed. A co-pumped ytterbium doped fiber amplifier was built with 10 μm core and 125 μm cladding (10/125 Nufern) fiber, as shown in Figure 3. Consequently, the (single-frequency) fiber amplifier was externally phase modulated using a frequency signal generator. SBS suppression was examined for various modulation frequencies and modulation depths, as plotted in Figure 2 (red dots). Notably, the experimental (sinusoidal) phase modulation results agree well with the time-dependent SBS model developed.

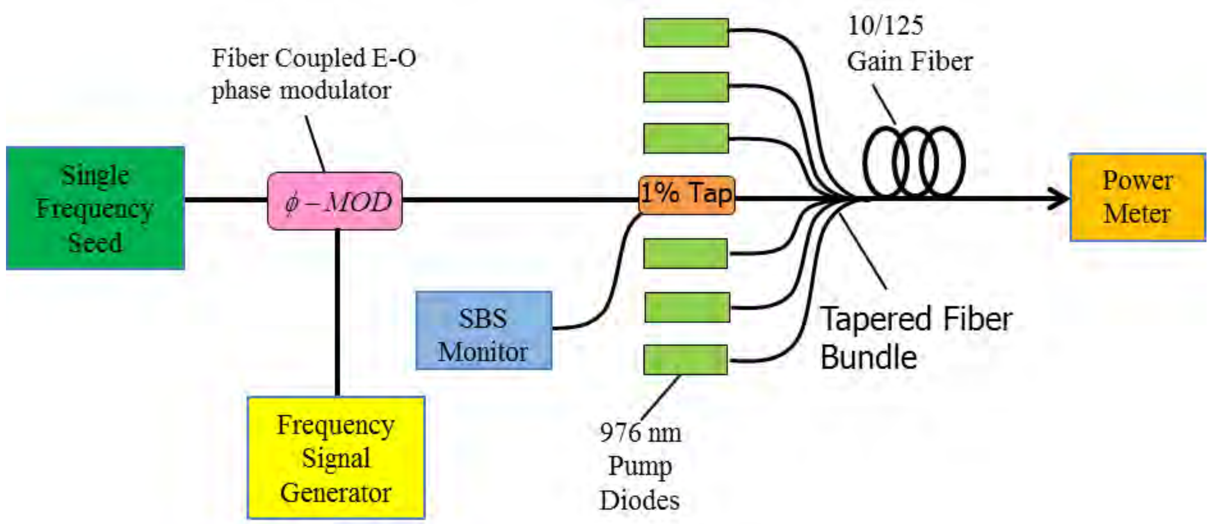

Figure 3. Schematic of phase modulated (Nufern 10/125) fiber amplifier with sinusoidal phase modulation applied and experimental results compared to time dependent SBS model (see Figure 2).

From Figure 2, we note that for modulation frequencies within the Brillouin bandwidth, $\omega_{FM}/\Gamma_B < 1$, little SBS enhancement is attained regardless of modulation amplitude due to a large degree of overlap between the SBS spectra in the sidebands. Accordingly, for the range of modulation frequencies, $0.5\Gamma_B \le \omega_{FM} \le 5\Gamma_B$, the SBS

threshold increases with modulation frequency. This regime also describes the transition from strong to weak overlap among the SBS in the optical sidebands. When considering even larger modulation frequencies, $\omega_{FM} > 5\Gamma_B$, additional enhancement in SBS suppression is minimal since in this regime the Brillouin gain overlap among the sidebands is very small. As expected, in the large modulation frequency limit, the threshold enhancement approaches the approximation of Eq. (17). It important to note that SBS threshold enhancement is not limited to ~4.25 times enhancement using sinusoidal phase modulation. According to Eq. (17), driving the phase modulation amplitude higher or increasing the modulation depth, γ, can further increase the SBS enhancement factor. As such, 7 times SBS enhancement was attained through sinusoidal phase modulation, primarily limited by the phase modulator's voltage handling capability.

4. SINUSOIDAL PHASE MODULATION (COHERENT BEAM COMBINING)

The major goal of linewidth broadening is SBS suppression. However, broadening to nanometer linewidths may hinder efficient beam combining in both coherent and spectrally beam combined systems. This is due to added path length complexities in CBC where the linewidth is inversely proportional to the temporal coherence of the laser ($L_c = c / n\pi\Delta\nu_l$). Likewise, spectral beam combining (SBC) using multi layered dielectric (MLD) gratings is linewidth sensitive and broader linewidths degrade combined beam quality. As a result, beam combining of narrow linewidth fiber lasers is essential for further power scaling to tens and hundreds of kilowatts. Here we aim to demonstrate CBC of fiber lasers via LOCSET [9]. Although LOCSET phase locking has been used extensively for single-frequency beam combining [10], LOCSET beam combining at narrow linewidths has not been demonstrated. As a result, we aim to combine 5 narrow linewidth, sinusoidal phase modulated elements using LOCSET.

The lasers are arranged in a tiled array pattern as shown in Figure 4. Subsequently, the master oscillator was (sinusoidal) modulated at a frequency, $\nu_{FM} = 900MHz$, and modulation depth, $\gamma = 1.435$. In order to preserve temporal coherence, fiber-coupled variable delay lines were used for path length matching of the lasers. Once path length matched, CBC of 5 narrow line lasers was achieved using LOCSET, as shown in Fig. 5. It is important note that due to the low fill factor ($\omega_0 / \Delta = 0.16$), substantial energy in the sidelobes is present. Nevertheless, high fringe visibility CBC using LOCSET phase locking is attained. We also note that beam combining at broader linewidths (~GHz) can also be implemented as long as the lasers remain path length matched.

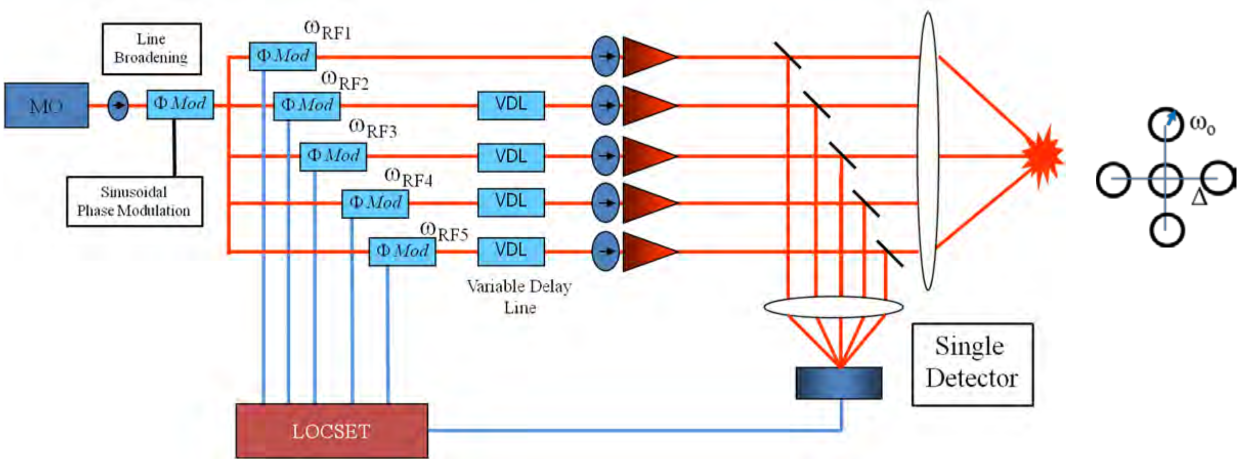

(a) (b)

Figure 4. a) Experimental arrangement for CBC of 5 sinusoidal phase modulated lasers in a b) tiled array configuration ($\omega_0 / \Delta = 0.16$).

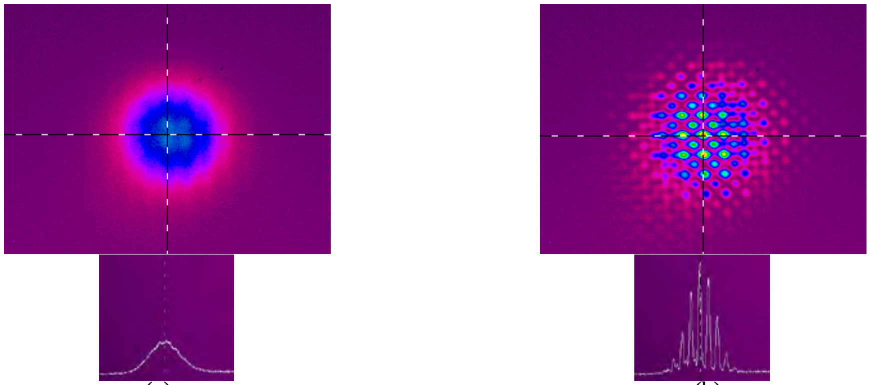

(a) (b)

Figure 5. a) Unlocked beam profile and b) 5 element narrow linewidth locked beam profile. Notably, high fringe visibility is attained.

5. CONCLUSION

In summary, we have developed a time-dependent model to study the effects of phase modulation on SBS. In this case, to experimentally validate the time-dependent model we considered only a single-sinusoidal phase modulation function. Notably, the SBS enhancement factor versus linewidth for different modulation depths was analyzed and good agreement between simulations and experimental results was achieved. Furthermore, narrow linewidth CBC of 5 sinusoidal phase modulated lasers was demonstrated via LOCSET. Consequently, we plan to extend the time-dependent model to analyze additional phase modulations schemes for efficient SBS suppression. We are currently examining white noise source and Psuedo Random Bit Sequence (PRBS) phase modulation through our nonlinear time-dependent model. More importantly, we believe our model offers a powerful tool for investigating the effects of SBS suppression in high-power fiber amplifiers.

ACKNOWLEDGEMENTS

This work was partially funded by the Air Force Office of Scientific Research (AFOSR).

5. REFERENCES

[1] J. P. Koplaw, D. Kliner, and L. Goldberg, "Single-mode operation of a coiled multimode fiber amplifier," Optics Letters **25**, 442-444 (2000).

[2] P. Mitchell, A. Janssen, and J. K. Luo, "High performance laser linewidth broadening for stimulated Brillouin suppression with zero parasitic amplitude modulation," Journal of Applied Physics **105**, 093104 (2009).

[3] Gabla, P.M., and Leclerc, E., "Experimental investigation of stimulated Brillouin scattering in ASK and DPSK externally modulated transmission systems," European Conf. Optical Commun., ECOC, ThC10-5, 657-660 (1993).

[4] G. D. Goodno, S. J. McNaught, J. E. Rothenberg, T. S. McComb, P. A. Thielen, M. G. Wickham, and M. E. Weber, "Active phase and polarization locking of a 1.4 kW fiber amplifier," Optics Letters **35**, 1542-1544 (2010).

[5] C. M. Zeringue and I. Dajani, "A theoretical investigation of stimulated Brillouin scattering in phase-modulated fiber amplifiers," Proceedings of SPIE Vol. **7836**, 7836O-1 (2010).

[6] R. W. Boyd, K. Rzaewshi, and P. Narum, "Noise initiation of stimulated Brillouin scattering," Physics Review A. **42**, 5514-5521 (1990).

[7] M. G. Raymer and J. Mostowski, "Stimulated Raman scattering: Unified treatment of spontaneous initiation and spatial propagation," Physic Review A **24**, 1980-1993 (1981).

[8] E. Lichtman, R. G. Waarts, and A. A. Friesem, "Stimulated Brillouin scattering excited by a modulated pump wave in single-mode fibers," Journal of Lightwave Technology **7**, 171-174 (1989).

[9] T. M. Shay, Vincent Benham, Mark A. Culpepper, D. Pilkington, Justin Spring, Douglas J. Nelson, and Chunte A. Lu, “First experimental demonstration of self-synchronous phase locking of an optical array,” Optics Express **14**, 12015-12021 (2006).
[10] A. Flores, T. M. Shay, C. A. Lu, C. Robin, B. Pulford, A. D. Sanchez, D. W. Hult, and K. B. Rowland, “Coherent Beam Combining of Fiber Amplifiers in a kW Regime,” *CLEO 2011*, Baltimore, MD, CF3.

DISTRIBUTION LIST

DTIC/OCP 8725 John J. Kingman Rd, Suite 0944 Ft Belvoir, VA 22060-6218	1 cy
AFRL/RVIL Kirtland AFB, NM 87117-5776	1 cy
Angel Flores Official Record Copy AFRL/RDLT	1 cy